

# Integrity Monitoring for GNSS Positioning Via Factor Graph Optimization In Urban Canyons

Weisong Wen, Qian Meng, and Li-Ta Hsu

*Interdisciplinary Division of Aeronautical and Aviation Engineering, The Hong Kong Polytechnic University*

## BIOGRAPHY

Weisong Wen received a Ph.D. degree in Mechanical Engineering from The Hong Kong Polytechnic University (PolyU), in Nov 2020. He was also a visiting Ph.D. student with the Faculty of Engineering, University California, Berkeley (UC Berkeley) in 2018. In 2020, he won the Best Presentation Award from the Institute of Navigation (ION), and the First Prize in Hong Kong Section in Qianhai-Guangdong-Macao Youth Innovation and Entrepreneurship Competition, 2019. Before joining PolyU as a Research Assistant Professor in April 2021, he was a senior research fellow at PolyU. His research interests include GNSS positioning, SLAM, and collaborative positioning in challenging environments autonomous driving vehicles, and unmanned aerial vehicles.

Dr. Qian MENG is currently an assistant professor in the School of Instrument Science and Engineering, Southeast University. He received his BEng degree in Automation and a Ph.D. degree in Control Science and Engineering from Nanjing University of Aeronautics and Astronautics, China, in 2013 and 2018, respectively. He was a visiting Ph.D. student at the Centre of Transport Studies, Imperial College London in 2017. After graduation, he worked as a postdoctoral fellow with the Department of Aeronautical and Aviation Engineering, Hong Kong Polytechnic University from 2019 to 2021. He joined Southeast University in Feb 2021. His current research interests focus on resilient and reliable navigation and positioning, GNSS receiver signal processing, and integrity for multi-sensor integration.

Li-Ta Hsu received the B.S. and Ph.D. degrees in aeronautics and astronautics from National Cheng Kung University, Taiwan, in 2007 and 2013, respectively. He is currently an assistant professor with the Interdisciplinary Division of Aeronautical and Aviation Engineering, The Hong Kong Polytechnic University, before he served as a post-doctoral researcher in the Institute of Industrial Science at the University of Tokyo, Japan. In 2012, he was a visiting scholar at University College London, the U.K. His research interests include GNSS positioning in challenging environments and localization for pedestrian, autonomous driving vehicle, and unmanned aerial vehicle

## ABSTRACT

Fault detection and exclusion (FDE) is significant for integrity monitoring of GNSS positioning for autonomous systems with navigation requirements. Moreover, the urban canyon scenario introduces additional challenges to the existing FDE for integrity monitoring, causing missed or false alarms, due to the significantly increased percentage of fault measurements. This paper proposed a sliding window aided FDE for GNSS positioning based on factor graph optimization (FGO) to alleviate these key issues. Different from the existing snapshot-based and the sequential-based (e.g. Extended Kalman filter) integrity monitoring methods where only the current or two consecutive epochs of measurements are considered in the FDE process, the proposed method in this paper improves the measurement redundancy with the help of the sliding window structure. Meanwhile, the GNSS measurements inside the sliding window are considered multiple times which enables the reconsideration of fault measurements. Moreover, the FGO employs multiple iterations and re-linearizations which improves the initial guess of the state estimation for FDE. The effectiveness of the proposed method is verified through a challenging dataset collected in urban canyons of Hong Kong using automobile-level low-cost GNSS receivers.

## 1. INTRODUCTION

The global navigation satellite system (GNSS) integrity, which was firstly developed in the aviation field, had recently attracted numerous attentions in the safe-critical transportation field in urban canyons, such as level-4 fully autonomous driving vehicles [1, 2]. It is defined as a measure of trust that can be placed in the correctness of the positioning information provided by the navigation system [3]. Generally, the GNSS integrity information can be provided in different manners. The most basic way is the GNSS navigation messages, which provide the anomalies information related to the navigation system and satellite operations

such as satellite clock errors. However, this kind of integrity information cannot be directly used in real-time applications as the ground control segment can take a few hours to figure out the potential anomalies. To this end, the receiver autonomous integrity monitoring (RAIM) technique was developed [4-6] continuously in the past several decades with a special focus on the aviation field. The first research stream is the snapshot algorithms such as least-squares residual-based RAIM [7] [8, 9]. The snapshot algorithm is generally based on the measurement residuals of the least-squares estimator. Meanwhile, only the measurements in a single epoch are considered [10]. The snapshot algorithm can effectively monitor the integrity of the GNSS positioning in the aviation field as only one fault is assumed and the variance of remaining GNSS measurements is known as zero-mean Gaussian distribution. However, this is not true for the case in urban canyons due to the numerous GNSS outlier measurements (e.g. multipath and non-line-of-sight receptions). In other words, multiple faults occur in urban canyons. Moreover, the navigation system usually involves multiple sensors (e.g. inertial navigation system, INS, LiDAR, camera) and the snapshot-based RAIM is not suitable. To fill this gap, the sequential approach was proposed which was based on the innovation of the Kalman filter [11] [12, 13]. Different from the snapshot-based approach, the sequential approach (e.g. Kalman filter-based) makes use of the measurements at the current epoch and the previous epoch. Moreover, the additional sensor could be employed to improve the fault detection and exclusion (FDE) performance [12, 13] under the sequential-based RAIM approach. However, the sequential-based RAIM approach relies heavily on the cost of the INS sensor and is significantly challenged in urban canyons with numerous multipath and NLOS receptions.

Our recent research in [14] showed that the factor graph-based GNSS/INS integration obtains better robustness against outlier measurements compared with the Kalman filtering. The major reason is that the factor graph could exploit the time-correlation between multiple epochs measurements simultaneously, with multiple linearizations and iterations properties. Theoretically, the factor graph considers the measurements in multiple epochs and involves a higher potential in detecting the fault measurements. Our very recent work in [15] also showed the advantage of factor graph optimization against the conventional Kalman filter-based approach in GNSS pseudorange/Doppler integration and GNSS real-time kinematic (GNSS-RTK) positioning. However, there is no existing work that specifically discusses the integrity of the factor graph-based GNSS positioning which considers the measurements in multiple epochs simultaneously. To fill this gap, in this paper, we proposed to study the integrity monitoring for GNSS positioning via factor graph optimization for the urban transportation application. Firstly, the GNSS pseudorange and Doppler measurements integration are integrated based on our previous work [15] using factor graph optimization. Meanwhile, we consider sliding window optimization which means measurements from the several epochs are considered simultaneously. Due to the superiority of the factor graph optimization, an improved GNSS positioning result is obtained compared with the conventional Kalman filter-based results which can provide a good initial guess to the FDE. Secondly, FDE is performed to remove the faulty measurements based on the residuals of the considered measurements via the chi-square test. Different from the snapshot or the sequential-based methods, the proposed FDE in this paper detects the faulty measurements based on the measurements inside a sliding window. To the best of the author's knowledge, this paper is the first work that studies the integrity monitoring of urban GNSS positioning via factor graph optimization.

The contributions of this paper are listed as follows:

- (1) This paper proposed to perform the fault detection and exclusion based on the measurements inside a sliding window to therefore increasing the data redundancy. Moreover, the sliding window-based FDE enables the reconsideration of the incorrect FDE.
- (2) This paper evaluates the performance of the proposed method using the dataset collected using a low-cost GNSS receiver.

The remainder of this paper is organized as follows. An overview of the proposed method is given in Section 2. The GNSS positioning using FGO is elaborated in Section 3. In Section 4, the proposed FDE considering the GNSS measurements inside the sliding window is presented. An experiment is performed to evaluate the effectiveness of the proposed method using a dataset collected in urban canyons of Hong Kong in Section 5. Finally, conclusions are drawn, and further work is presented in Section 6.

## 2. OVERVIEW OF THE PROPOSED METHOD

An overview of the method proposed in this paper is shown in Fig. 1. The system consists of two parts: (1) system state initialization corresponding to the left side of the figure. (2) system fault detection and exclusion corresponding to the right side of the figure. In the first part, the system state inside a given sliding window is initialized by solving the FGO problem by considering all the GNSS measurements associated with the sliding window, including the pseudorange and Doppler measurements (see Fig. 1-(a)). An illustration of the FGO is shown in Fig. 1-(c). The black satellite icon denotes the healthy satellite measurement, such as the line-of-sight (LOS) satellite. The red satellite icon denotes the polluted satellite measurements, such as the non-line-of-sight (NLOS) measurement. In the second part, the FDE is performed iteratively based on all the GNSS

measurements inside the sliding window. An illustration of the graph structure after applying the FDE is shown in Fig. 1-(d) where all the GNSS measurements inside the window are considered and only the black satellite (LOS) survives from the FDE.

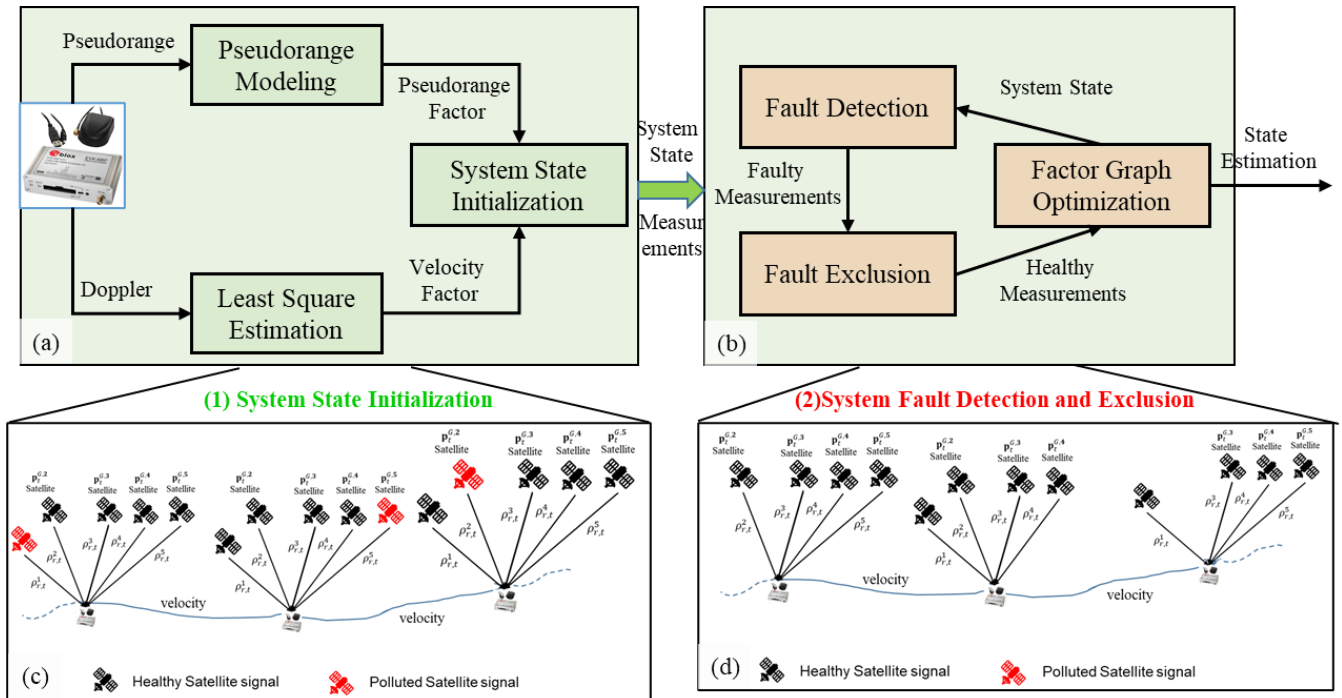


**Fig. 1. Overview of the proposed method which mainly includes the system state initialization and system fault detection and exclusion.**

### 3. SYSTEM STATE INITIALIZATION VIA PSEUDORANGE/DOPPLER FUSION USING FGO

This system state inside a sliding window is initialized by solving the FGO problem by considering all the GNSS measurements associated with the sliding window, including the pseudorange and Doppler measurements. The FGO problem is formulated and solved based on our previous work in [16]. The state of the GNSS receiver is represented as follows [16]:

$$\boldsymbol{\chi} = [\mathbf{x}_{r,1}, \mathbf{x}_{r,2}, \dots, \mathbf{x}_{r,n}] \quad (1)$$

$$\mathbf{x}_{r,t} = (\mathbf{p}_{r,t}, \mathbf{v}_{r,t}, \delta_{r,t})^T \quad (2)$$

where the variable  $\boldsymbol{\chi}$  denotes the set states of the GNSS receiver from the first epoch to the current  $n$ . The  $\mathbf{x}_{r,t}$  denotes the state of the GNSS receiver at epoch  $t$  which involves the position ( $\mathbf{p}_{r,t}$ ), velocity ( $\mathbf{v}_{r,t}$ ) and receiver clock bias ( $\delta_{r,t}$ ). The objective function for the GNSS positioning using FGO is formulated as follows:

$$\boldsymbol{\chi}^* = \arg \min_{\boldsymbol{\chi}} \sum_{s,t} \|e_{r,t}^{DV}\|_{\sigma_{r,t}^{DV}}^2 + \|e_{r,t}^S\|_{\sigma_{r,t}^S}^2 \quad (3)$$

The variable  $\boldsymbol{\chi}^*$  denotes the optimal estimation of the state sets, which can be estimated by solving the objective function (3). The  $e_{r,t}^{DV}$  denotes the residual function associated with the Doppler velocity factor. The  $e_{r,t}^S$  denotes the residual function associate with the pseudorange factor. The detail of the formulation for both the Doppler velocity and pseudorange factors can be found in [16].

### 4. FAULT DETECTION AND EXCLUSION

This section presents the fault detection and exclusion based on the state initialization in Section 3. Since the Doppler measurement is less sensitive to the impacts on multipath and NLOS receptions, this paper only considers the faults in the pseudorange measurements. After solving equation (3), the residual associated with the epoch  $t$  can be denoted as follows:

$$\mathbf{e}_{r,t} = (e_{r,t}^1, \dots, e_{r,t}^S)^T \quad (4)$$

where the variable  $S$  denotes the number of pseudorange measurements at the given epoch  $t$ . Then the normalized residuals can be formulated as follows:

$$\tilde{\mathbf{e}}_{r,t} = (\mathbf{e}_{r,t}^1 / \sigma_{r,t}^1, \dots, \mathbf{e}_{r,t}^S / \sigma_{r,t}^S)^T \quad (5)$$

Considering the measurements inside a sliding window with a size of  $M$  epochs, the normalized residuals can be denoted as follows:

$$\tilde{\mathbf{e}}_M = (\tilde{\mathbf{e}}_{r,1}, \dots, \tilde{\mathbf{e}}_{r,t})^T \quad (6)$$

An illustration of the sliding window can be seen in Fig. 2. Therefore, the test statistics of the residuals can be formulated as follows:

$$\Psi_M = \tilde{\mathbf{e}}_M^T \tilde{\mathbf{e}}_M \quad (7)$$

The  $\Psi_M$  denotes the chi-square statistics [17]. To identify the existence of the outlier measurements, the  $\Psi_M$  is compared with a threshold calculated using a one-tailed Chi-square distribution based on a significance level and degree of freedom as follows:

$$\Psi_M < \mathcal{H}_{\alpha,m}^2 \quad (8)$$

where the variable  $\alpha$  denotes the significance level which is set to 0.001 in this paper, which indicates a 99.9% confidence level. The variable  $m$  denotes the degree of freedom of the chi-square distribution. If the test succeeds, the estimated state is the final state estimation which is free of fault. Otherwise, the pseudorange factor with the largest normalized residual is to be excluded from the factor graph. For example, the red satellite in Fig. 2 is excluded and the FGO (see equation (3)) is performed again based on the remaining GNSS measurements until the test (see equation (8)) succeeds. The top panel of Fig. 2 shows the snapshot-based outlier detection which only considers the GNSS measurements at the current epoch. The bottom panel shows the outlier detection considering the GNSS measurements inside a sliding window (see the light blue box). Specifically, the snapshot-based outlier detection is a special case of the sliding window-based method where the size of the window is 1 epoch only.

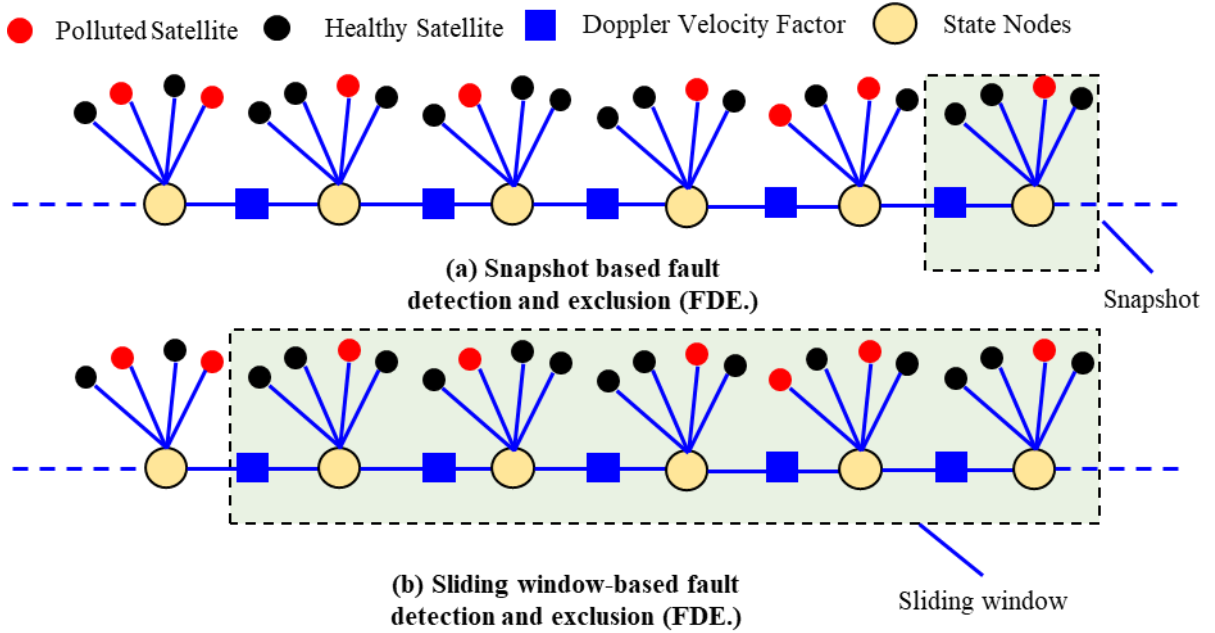


Fig. 2. Demonstration of the FDE for both the snapshot-based and sliding window-based methods.

## 5. EXPERIMENTAL RESULTS AND DISCUSSION

### 5.1 Experimental Setup

To verify the effectiveness of the proposed method, we collect the dataset in a typical urban scene of Hong Kong. Fig. 3 shows the data collection vehicle installed with multiple sensors. Meanwhile, the tested scene is shown in Fig. 4 which involves buildings and trees which is challenging for the GNSS positioning. In the experiment, a u-blox M8T GNSS receiver was used to collect raw GPS/BeiDou measurements at a frequency of 1 Hz. In addition, the NovAtel SPAN-CPT, a GNSS (GPS, GLONASS, and Beidou) RTK/INS (fiber-optic gyroscopes, FOG) integrated navigation system was used to provide ground truth of

positioning. The gyro bias in-run stability of the FOG is 1 degree per hour, and its random walk is 0.067 degrees per hour. The baseline between the rover and the GNSS base station is about 5 km. All the data were collected and synchronized using a robot operation system (ROS) [18]. The coordinate systems between all the sensors were calibrated before the experiments.

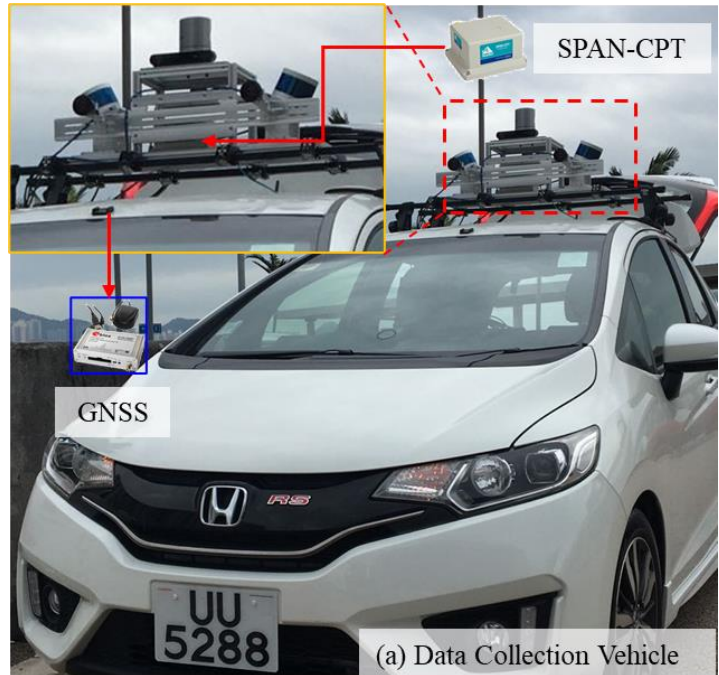


Fig. 3. Illustration of the data collection vehicle.



Fig. 3. Illustration of the tested scenario in an urban canyon of Hong Kong.

We analyzed the performance of GNSS positioning aided by snapshot-based FDE and sliding window-based FDE. The accuracy is evaluated in the ENU frame by selecting the first point as the reference position.

- (a) **FGO** [16]: The system is initialized by the FGO (see equation (3)).
- (b) **FGO-FDE-Snapshot**: The system is initialized by the FGO (see equation (3)). Then the FDE is performed in the current epoch (see top panel of Fig. 2) iteratively until the test statistic satisfied the (8).
- (c) **FGO-FDE-SW**: The system is initialized by the FGO (see equation (3)). Then the FDE is performed considering the GNSS pseudorange measurement inside a sliding window (see bottom panel of Fig. 2) iteratively until the test statistic satisfied the (8). The “SW” indicates the sliding window. Specifically, we also compare the performance of the FGO-FDE-SW under different sizes concerning the sliding window to further show the impacts of the selection of window size.

### 6.2 Performance Evaluation in Urban Canyon

The results of the above-mentioned three methods are shown in Table 1. A mean error of 4.25 meters is obtained using the FGO based on our previous work in [16] with a maximum error of 8.38 meters. After applying the snapshot-based FDE method, the mean error decreases to 3.67 meters which shows that the FDE can help to excludes the potential outlier measurements to, therefore, improve the overall positioning accuracy. After applying the proposed sliding window-based FDE with a window size of 15, the mean error decreases to 3.35 meters. The improvement compared with the snapshot-based FDE is due to the increased

data redundancy which also enables the reconsideration of the fault decisions. The trajectories of the listed three methods are shown in Fig. 4. The errors during the experiments are shown in Fig. 4. It can be seen that the blue curve (proposed method) is almost always below the green curve (the snapshot-based FDE) which shows the effectiveness of the proposed method. However, we can see that the overall improvement from the proposed method is still limited. One of the major reasons is that the fault exclusion logic that the measurement with the largest normalized residual is excluded. In the real case, the GNSS measurement with the largest residual may not necessarily indicate the faulty measurements. One of the potential solutions is to find the faulty measurements by excluding each of the measurements inside the sliding window to find the most consistent set of the GNSS measurements set. However, this can cause a significantly higher computation load and this will be one of our future work.

**Table 1. Positioning performance comparison.**

Items	FGO (m)	FGO-FDE-Snapshot (m)	FGO-FDE-SW-15 (m)
<b>Mean error</b>	4.25	3.67	3.35
<b>STD</b>	1.98	1.96	2.08
<b>Maximum error</b>	8.38	8.43	8.47

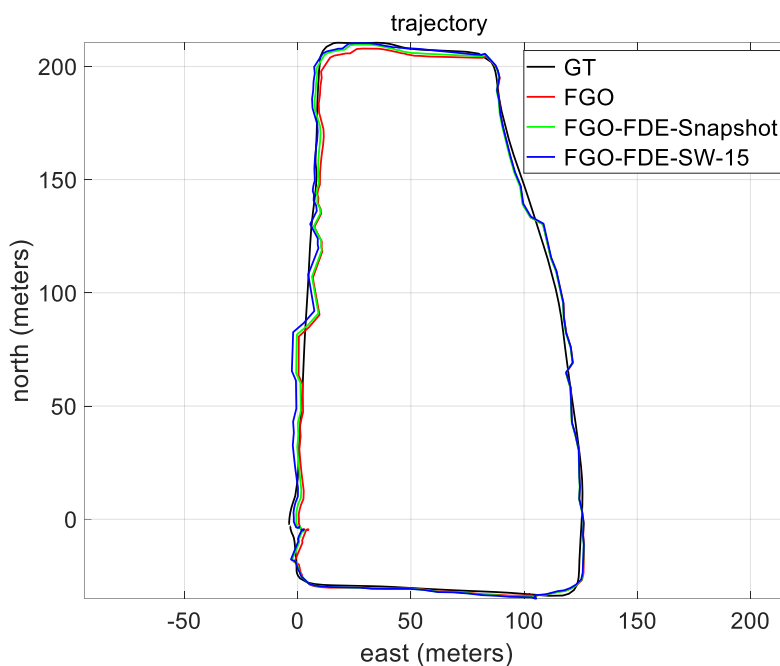


**Fig. 4. Trajectories of the evaluated methods. The black curve denotes the ground truth (GT). The red, green, and blue curves denote the solutions from FGO, FGO-FDE-Snapshot, and FGO-FDE-SW with a window size of 15, respectively.**

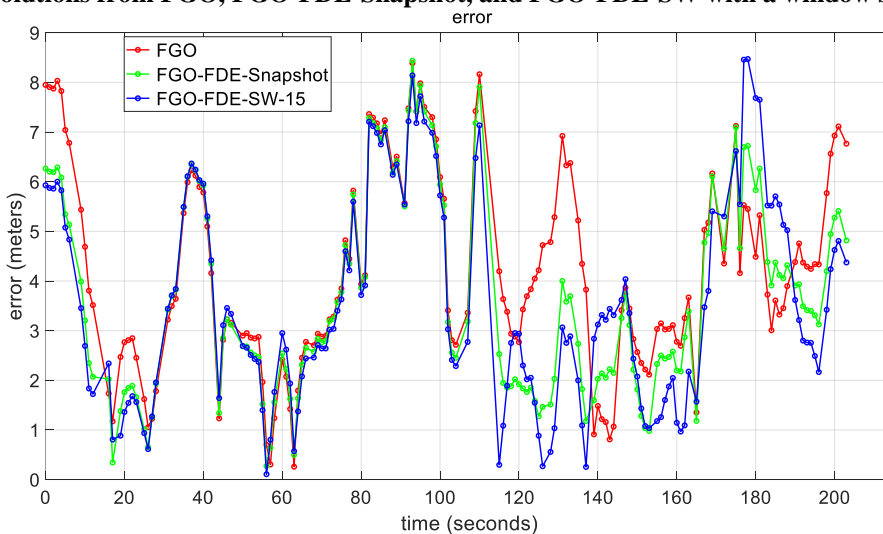


**Fig. 5. Errors of the evaluated methods. The red, green, and blue curves denote the solutions from FGO, FGO-FDE-Snapshot, and FGO-FDE-SW with a window size of 15, respectively.**

As shown in Table 1, the proposed (FGO-FDE-SW) method with a window size of 15 leads to improved positioning accuracy. It is interesting to see how the proposed method works under different window sizes. To this end, we present the error cumulated distribution function (ECDF) of the proposed method with window sizes of 5, 10, 15, and 20 in Fig. 6, respectively. Overall, the positioning accuracy improved gradually with the increased window size which can see by comparing the FGO-FDE-SW-5 and FGO-FDE-SW-15. This is caused by the increased data redundancy which again shows the effectiveness of the proposed method. However, similar positioning accuracy is achieved after increasing the window size from 15 to 20. One of the reasons is that the time correlation between the measurements from the current epoch and the first epoch is small. In the future, we will study the quantification of the time correlation between multiple epochs of states.

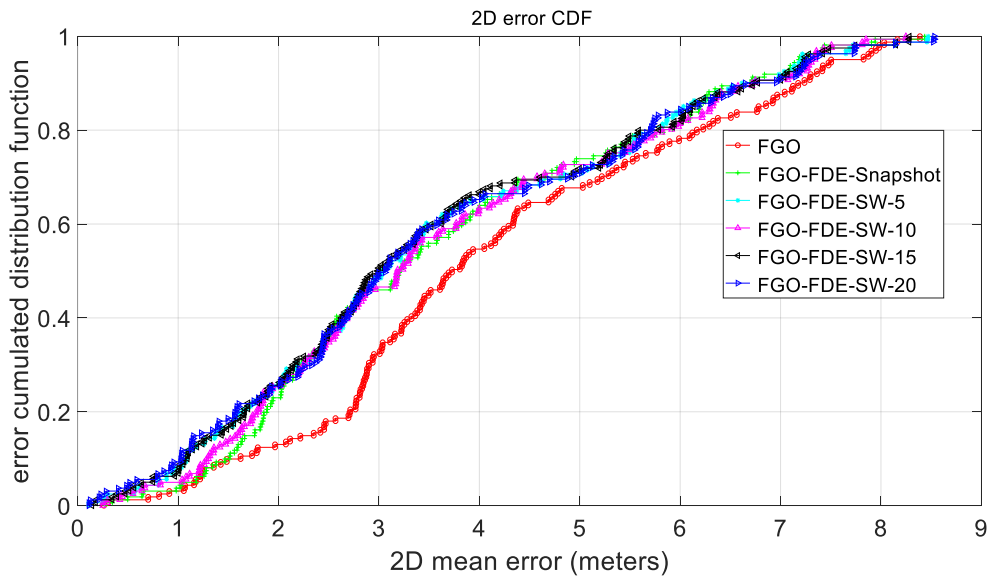


**Fig. 6. Errors of the FGO-FDE-SW under different window sizes. The more upper left the better.**

## 6. CONCLUSIONS AND FUTURE WORK

Fault detection and exclusion (FDE) is significant for integrity monitoring of GNSS positioning for autonomous systems with navigation requirements. This paper proposed a sliding window aided FDE for GNSS positioning based on factor graph optimization (FGO) to alleviate these key issues. The sliding window-based FDE increases the data redundancy and also enables the reconsideration of the faulty measurements. The evaluated dataset shows that the proposed FDE methods can help to improved the positioning accuracy. Moreover, the improvement is enhanced with the increased window size.

The removed outliers inside the current sliding window are not considered in the next window and the consideration of those prior outlier measurements will be considered in future work. Moreover, the protection level of the integrity will also be calculated based on the proposed sliding window FDE in the future. The urban scenarios introduce increased challenges to FDE. Employing the additional sensors [19-21] to detect the potential GNSS outlier measurements to improve the integrity monitoring will also be investigated in the future.

## REFERENCES

- [1] G. Wan *et al.*, "Robust and precise vehicle localization based on multi-sensor fusion in diverse city scenes," in *2018 IEEE International Conference on Robotics and Automation (ICRA)*, 2018: IEEE, pp. 4670-4677.
- [2] W. Wen *et al.*, "Urbanloco: a full sensor suite dataset for mapping and localization in urban scenes," in *2020 IEEE International Conference on Robotics and Automation (ICRA)*, 2020: IEEE, pp. 2310-2316.
- [3] P. B. Ober, "Integrity prediction and monitoring of navigation systems," 2004.

- [4] Y. C. Lee, "Analysis of range and position comparison methods as a means to provide GPS integrity in the user receiver," in *Proceedings of the 42nd Annual Meeting of The Institute of Navigation (1986)*, 1986, pp. 1-4.
- [5] R. G. Brown and P. W. McBurney, "Self-Contained GPS Integrity Check Using Maximum Solution Separation," *Navigation*, vol. 35, no. 1, pp. 41-53, 1988.
- [6] M. Brenner, "Implementation of a RAIM Monitor in a GPS Receiver and an Integrated GPS/IRS," in *Proceedings of the 3rd International Technical Meeting of the Satellite Division of The Institute of Navigation (ION GPS 1990)*, 1990, pp. 397-414.
- [7] T. Walter and P. Enge, "Weighted RAIM for precision approach," in *PROCEEDINGS OF ION GPS*, 1995, vol. 8, no. 1: Institute of Navigation, pp. 1995-2004.
- [8] R. G. Brown, "A baseline GPS RAIM scheme and a note on the equivalence of three RAIM methods," *NAVIGATION, Journal of the Institute of Navigation*, vol. 39, no. 3, pp. 301-316, 1992.
- [9] R. S. Young, G. A. McGraw, and B. T. Driscoll, "Investigation and comparison of horizontal protection level and horizontal uncertainty level in FDE algorithms," in *Proceedings of the 9th International Technical Meeting of the Satellite Division of The Institute of Navigation (ION GPS 1996)*, 1996, pp. 1607-1614.
- [10] L.-T. Hsu, H. Tokura, N. Kubo, Y. Gu, and S. Kamijo, "Multiple faulty GNSS measurement exclusion based on consistency check in urban canyons," *Ieee Sens J*, vol. 17, no. 6, pp. 1909-1917, 2017.
- [11] M. Joerger and B. Pervan, "Integrity risk of Kalman filter-based RAIM," in *Proceedings of the 24th International Technical Meeting of The Satellite Division of the Institute of Navigation (ION GNSS 2011)*, 2011, pp. 3856-3867.
- [12] Ç. Tanıl, S. Khanafseh, M. Joerger, and B. Pervan, "Kalman filter-based INS monitor to detect GNSS spoofers capable of tracking aircraft position," in *2016 IEEE/ION Position, Location and Navigation Symposium (PLANS)*, 2016: IEEE, pp. 1027-1034.
- [13] O. G. Crespillo, A. Grosch, J. Skaloud, and M. Meurer, "Innovation vs residual KF based GNSS/INS autonomous integrity monitoring in single fault scenario," in *Proceedings of the 30th International Technical Meeting of the Satellite Division of The Institute of Navigation (ION GNSS+ 2017)*, 2017, pp. 2126-2136.
- [14] Y. C. K. Weisong Wen, Li-Ta Hsu, "Performance Comparison of GNSS/INS Integrations Based on EKF and Factor Graph Optimization," presented at the ION GNSS+ 2019, Florida, 2019.
- [15] N. Wen W., HF., Hsu, L.T., "GraphGNSSLib: An Open-source Package for GNSS Positioning and Real-time Kinematic Using Factor Graph Optimization (submitted)," *Gps Solut*, 2020.
- [16] W. Wen and L.-T. Hsu, "Towards Robust GNSS Positioning and Real-time Kinematic Using Factor Graph Optimization," *arXiv preprint arXiv:2106.01594*, 2021.
- [17] C.-Y. Chi, C.-H. Chen, C.-C. Feng, and C.-Y. Chen, "Fundamentals of statistical signal processing," *Blind Equalization and System Identification: Batch Processing Algorithms, Performance and Applications*, pp. 83-182, 2006.
- [18] M. Quigley *et al.*, "ROS: an open-source Robot Operating System," in *ICRA workshop on open source software*, 2009, vol. 3, no. 3.2: Kobe, Japan, p. 5, doi: <http://www.cim.mcgill.ca/~dudek/417/Papers/quigley-icra2009-ros.pdf>.
- [19] W. Wen, G. Zhang, and L.-T. Hsu, "GNSS NLOS exclusion based on dynamic object detection using LiDAR point cloud," *Ieee T Intell Transp*, 2019.
- [20] W. Wen, G. Zhang, and L. T. Hsu, "Correcting NLOS by 3D LiDAR and building height to improve GNSS single point positioning," *Navigation*, vol. 66, no. 4, pp. 705-718, 2019, doi: <https://doi.org/10.1002/navi.335>.
- [21] W. Wen, X. Bai, Y.-C. Kan, and L.-T. Hsu, "Tightly Coupled GNSS/INS Integration Via Factor Graph and Aided by Fish-eye Camera," *Ieee T Veh Technol*, 2019, doi: 10.1109/TVT.2019.2944680.